Optics and Lasers in Engineering 102 (2018) 126–135

Contents lists available at ScienceDirect

Optics and Lasers in Engineering

journal homepage: www.elsevier.com/locate/optlaseng

Smartphone based scalable reverse engineering by digital image correlation

Amey Vidvans, Saurabh Basu*

Harold and Inge Marcus Department of Industrial and Manufacturing Engineering, Pennsylvania State University, University Park, PA, USA

A B S T R A C T

There is a need for scalable open source 3D reconstruction systems for reverse engineering. This is because most commercially available reconstruction systems are capital and resource intensive. To address this, a novel reconstruction technique is proposed. The technique involves digital image correlation based characterization of surface speeds followed by normalization with respect to angular speed during rigid body rotational motion of the specimen. Proof of concept of the same is demonstrated and validated using simulation and empirical characterization. Towards this, smart-phone imaging and inexpensive off the shelf components along with those fabricated additively using poly-lactic acid polymer with a standard 3D printer are used. Some sources of error in this reconstruction methodology are discussed. It is seen that high curvatures on the surface suppress accuracy of reconstruction. Reasons behind this are delineated in the nature of the correlation function. Theoretically achievable resolution during smart-phone based 3D reconstruction by digital image correlation is derived.

1. Introduction

Recent advances in additive manufacturing (AM) have enabled shorter product development times by accelerating fabrication of prototypes featuring complex geometries [1,2]. This facilitates production of desired shapes at rates that are unmatched by conventional scalable fabrication routes. Further, AM has been envisioned as an approach to reverse engineering involving rebuild and repair of complex broken machine components in small volumes [3]. This methodology towards equipment repair is highly useful in isolated environments where access to conventional machine tools and other fabrication equipment is not available [4]. Towards this, stand alone 3D-printers based on polymer [5–7], metallic [8–10] and ceramic material systems [11–13] have been developed.

A crucial aspect in the reverse engineering of complex shapes for repair is the characterization, *i.e.* 3D-reconstruction of component geometries. Traditional approaches towards the same have utilized contact (*e.g.* coordinate measuring machine) and non-contact (*e.g.* optical laser scanning and computed tomography) approaches. These approaches involve the detection of edges by electro-mechanical or photo-electronic methods. In this regard, these 3D-reconstruction techniques rely on expensive and often unwieldy pieces of equipment akin to conventional machine tools, wherein the utility of AM processes for 3D-printing based repair is subdued.

Attempts towards mitigation of these shortcomings have looked at structure from motion (SfM) based optical photogrammetric range imaging for 3D-reconstruction [14]. This technique involves imaging of the object of interest from multiple overlapping angles followed by detection of common features across these images. Subsequently, the movement of these features across images is correlated with the corresponding motion of the camera, wherein the features are eventually mapped onto a 3D space representative of the shape of the original object. In this regard, a concomitant and accurate characterization of the camera motion is crucial for successful implementation of SfM algorithms. However, this characterization is complicated by noise and drift in the inertial measurement units and camera motion sensors, thus resulting in form and dimension errors in the reconstructed shape. The characterization of camera motion is therefore often performed via image processing by tracking strategically placed or a-priori identified high contrast features on the object of interest [14,15]. Alternatively, imaging for 3D reconstruction has also been performed at fixed points in space, wherein the camera poses were controllably varied resulting in its motion across images being delineated a-priori [16].

The accuracy of the aforementioned reconstruction methodologies monotonically depends on the number of input images [17]. Providing several hundred images as input can result in dense point clouds upon reconstruction, wherein high fidelity can be achieved in reverse engineering of complex geometries. This is because the density of point clouds directly governs the voxel resolution at which the reconstructed shape can be fabricated additively. Unfortunately, manual acquisition of several hundred images of the same object is a challenging task. Towards this, fixing hundreds of points in space for imaging to achieve a-priori delineation of camera motion can naturally result in measurement errors. This challenge can be further exacerbated during reconstruction of small objects while acquiring high-resolution, *i.e.* closeup images that contain non-redundant information.

Alternative routes towards reconstruction of topographies have looked at structured light profilometry [18]. This technique relies on projection of fringes, *i.e.* spatially varying dark/bright/colored light strips onto 3D shapes [19]. Upon incidence on the surface, these fringes

* Corresponding author.
E-mail addresses: sxb514@psu.edu, sxb514@engr.psu.edu (S. Basu).

https://doi.org/10.1016/j.optlaseng.2017.11.004
Received 28 July 2017; Received in revised form 29 September 2017; Accepted 8 November 2017
0143-8166/

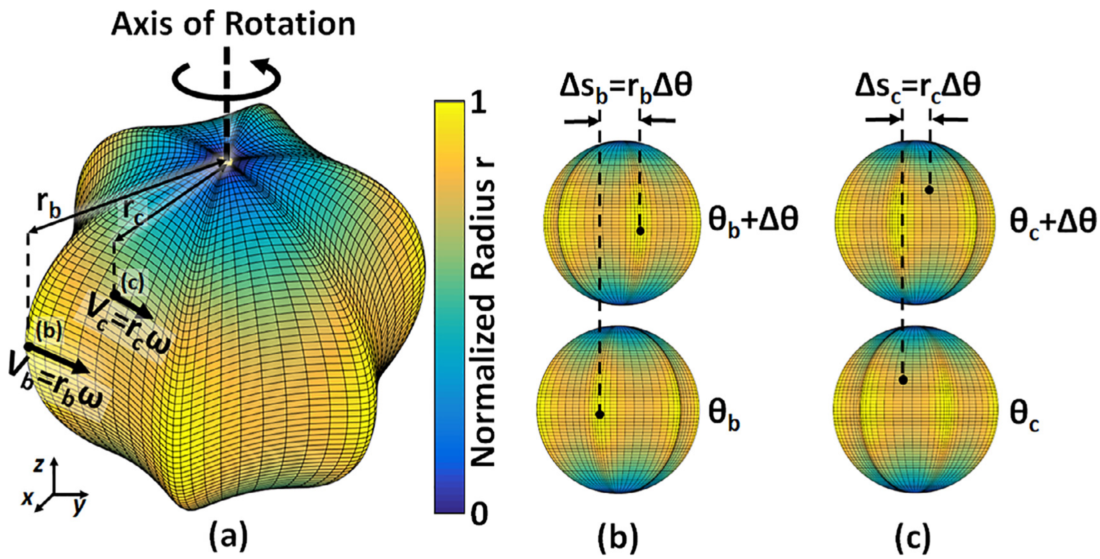

Fig. 1. 3D-Reconstruction by rigid body rotational transformation of object. (a) Non-speherical shape featuring gradient in radii with respect to axis of rotation. A larger radius r_b results in larger velocity $V = r_b\omega$ and larger displacement $\Delta s_b = r_b\Delta\theta$ for the same angular velocity ω and angle of rotation $\Delta\theta$, respectively, as shown in (b), compared to a smaller radius r_c (c).

get distorted, characteristics of which are governed locally by their projection angle, curvature of the surface and phase associated with the fringe pattern [20]. This distortion can be analyzed to reproduce the real 3D shape of the specimen of interest. Structured light profilometry also known as fringe projection profilometry is traditionally performed using a kinect camera along with software based processing in photographic [21] and video-modes [22]. Recently proposed variants of this approach have attempted to characterize large enclosed regions of cylindrical spaces [23]. Further, the approach has found utility in high-fidelity characterization of micro-meter sized features [24].

In the present research, we propose a novel route to shape characterization using smart-phone based 3D-reconstruction. This route utilizes rigid body rotational transformation of the component shape of interest, wherein original points on the surface of the shape are mapped onto a 3D space. While sharing similarities with the original family of SfM algorithms, our approach involves imposition of rigid-body rotational motion to the component using a stage fabricated in-house using in-expensive off-the-shelf components. This stage is light/portable and the methodology relies on smart-phone imaging. In this regard, this methodology can be used to perform high-fidelity 3D-characterization when access to high-accuracy instrumentation is restricted. Details of this stage are described in the forthcoming sections. It is envisioned that this methodology will augment reverse engineering capabilities of AM platforms by providing accurate 3D-reconstruction using inexpensive open source components.

2. Principals of 3D-reconstruction using a smart-phone and digital image correlation

2.1. Measuring principals

The concept underlying our proposed methodology for 3D reconstruction is illustrated in Fig. 1. Fig. 1a shows an arbitrary non-spherical shape that is rotated about an axis, wherein the color illustrates the normalized radius of points on the surface. During rotation at angular speed ω, points further away from this axis feature a larger surface speed as governed by:

$$||\vec{V}|| = ||\vec{r} \times \vec{\omega}|| \tag{1}$$

Consequently, these points exhibit a larger displacement for angular displacement $\Delta\theta$ as prescribed by:

$$\Delta s = r\Delta\theta \tag{2}$$

This feature is evident upon comparison of points b and c in Fig. 1, these exhibiting larger, *i.e.* r_b, and smaller *i.e.* r_c, radii with respect to the axis of rotation, respectively. Upon rotation through an angle $\Delta\theta$, the point b moves a larger distance $\Delta s_b = r_b\Delta\theta$, in comparison with the corresponding distance $\Delta s_c = r_c\Delta\theta$. In this regard, the crux of the proposed approach to 3D-reconstruction lies in the delineation of the aforementioned displacement Δs from the sequence of digital images of the rigid body rotation process. An approach towards this characterization is described in Section 2.2.

2.2. Digital image correlation algorithm

Characterization of displacement of points on the surface of arbitrary objects undergoing rigid body rotation was performed using digital image correlation (DIC). This involves recording the rotation process in a sequence of digital images. Subsequently, motion of asperities or high-contrast features on the surface of the rotating object is delineated using image correlation algorithms [25,26]. This motion is then normalized with respect to the angular rotation speed in order to characterize the radius of the corresponding point with respect to the axis of rotation as prescribed in the Section 2.1. Fig. 2 illustrates the characterization of displacement fields using DIC. Herein, Fig. 2a represents an arbitrary asperity field containing high contrast features, whereas Fig. 2b shows the same field artificially displaced to the right by $(\Delta u_0, \Delta v_0) = (15, 0)$ pixels. In order to characterize this displacement, a template demarcated within the dashed square in Fig. 2a is selected. Subsequently, the correlation coefficient field associated with this template and the final image is characterized as [27,28]:

$$\gamma(x, y) = \frac{\Sigma_{u,v}\left[f(x+u, y+v) - \bar{f}_{x,y}\right]\left[t(u,v) - \bar{t}\right]}{\left(\Sigma_{u,v}\left[f(x+u, y+v) - \bar{f}_{x,y}\right]^2 \Sigma_{u,v}\left[t(u,v) - \bar{t}\right]^2\right)^{0.5}} \tag{3}$$

Here, x and y refer to the displacement of Fig. 2b with respect to Fig. 2a. Further, $\bar{t} = \frac{\Sigma_{u=0,v=0}^{T_x,T_y} t(u,v)}{T_x T_y}$ is the mean intensity of the template demarcated in Fig. 2a, where T_x and T_y refer to dimensions of this template along the horizontal, *i.e.* x and vertical, *i.e.* y directions, respectively. Finally, $\bar{f}_{x,y} = \frac{\Sigma_{u=0,v=0}^{T_x,T_y} f(x+u,y+v)}{T_x T_y}$ is the mean intensity of the offset image, *i.e.* Fig. 2b, calculated at location (x, y) over a zone featuring the same dimensions as the template, *i.e.* T_x, T_y. The denominator in the aforementioned formula for cross correlation $\gamma(x, y)$ refers to the corresponding standard deviations. The normalization of $\gamma(x, y)$ with respect